

# Selective photochemistry via adiabatic passage: An extension of stimulated Raman adiabatic passage for degenerate final states

Mark N. Kobrak and Stuart A. Rice

*The Department of Chemistry and the James Franck Institute, The University of Chicago, Chicago, Illinois 60637*

(Received 24 September 1997)

In this paper we extend the existing theory of stimulated Raman adiabatic passage (StiRAP) in three-level systems to examine the nature of selective photoexcitation using counterintuitively ordered pulses. Our goal is to develop a version of StiRAP that permits control of product selectivity in a chemical reaction. We analyze the case of selective excitation to one state in a pair of degenerate target states in a four-level system, and find that one cannot control the ratio of the populations in the two states in a resonant two-photon process. However, the extension of the system to include a fifth state and a third laser field makes selective excitation to one of the degenerate states possible. It is found that, subject to reasonable restrictions, one may accomplish complete population transfer to a single target state of a degenerate pair of states in a five-level system.

[S1050-2947(98)03804-9]

PACS number(s): 33.80.Be, 42.50.Vk

## I. INTRODUCTION

There has recently been considerable interest in applying adiabatic passage excitation to three-level systems. It has been found that one may use a “counterintuitively” ordered pair of overlapping light pulses (i.e., with Stokes pulse preceding pump pulse) to access a trapped eigenstate of the dressed Hamiltonian. This eigenstate has a node in the intermediate level, so when excitation is complete all population is transferred to the target state with no loss to the intermediate state [1]. A sizable body of theoretical literature on the subject now exists [1–9], and experiments [10–12] have confirmed the validity of the approach.

Since its discovery, there have been a number of papers extending StiRAP to multilevel systems. Shore and co-workers [2], and later Tannor [3], developed methods for population transfer in systems consisting of initial and final states that are coupled by an arbitrarily long chain of intermediate states. It is found in both cases that complete population transfer is possible in such a system, provided that the chain includes an odd number of states. Oreg and co-workers [4] have found it is possible to use a StiRAP-like excitation process in a four-level chain, suggesting that the technique is not limited to chains with an odd number of levels, but as yet there have been no more general studies of chains with an even number of levels. In a somewhat different vein, Coulston and Bergmann [5] have studied the case of four- and five-level “branched” systems, in which at least one state is coupled to three or more other states (i.e., the states cannot be described by a single chain). And Bergmann and co-workers [6,11] recently demonstrated that it is possible to transfer population through specific pathways of a more complicated branched state structure.

Our goal in this work is to examine StiRAP-like excitation processes in the context of photoselectivity, i.e., control of product selectivity in a chemical reaction. The selective excitation of a single state has been studied extensively in other contexts [13], but to date there has been little work

done connecting these approaches with recent work on StiRAP and its variants. The emphasis has so far been on demonstrating that the counterintuitive pulse sequence used in StiRAP represents the solution to an optimal control problem, a question addressed by Band and Magnes [8] and resolved by Malinovsky and Tannor [3]. The goal of this work is somewhat different: We ask whether one may use a StiRAP-like process to achieve selective population transfer in a multilevel system.

We find that it is possible to take advantage of the symmetries of multilevel systems to selectively excite specific pathways. We treat the case of a pair of degenerate target states, and show that while a counterintuitive excitation scheme in a four-level system cannot produce relative populations in the two states that differ from those obtained in conventional two-photon excitation, it is possible to use coupling to a fifth state to change the population ratio and, in certain circumstances, even achieve 100% population transfer to a single state of the degenerate pair regardless of the relative transition dipole moments for excitation of those states from the ground state. We conclude with an examination of how one might apply the scheme described to a molecular system.

## II. THREE-LEVEL SYSTEMS

### A. Eigenstates of the ladder system

We begin by examining a sample three-level system, the ladder configuration shown in Fig. 1. The system consists of a ground state, an intermediate state, and a final state in which we wish to maximize the population. These matter eigenstates are coupled by the effects of two electric fields; the field that is resonant with the transition from the ground to the intermediate state will be referred to as the pump field, and the field that is resonant with the intermediate-to-finalstate transition will be labeled the Stokes field, in analogy with Raman processes. The Hamiltonian for such a system is then

$$\mathbf{H} = \frac{1}{2} \begin{pmatrix} 2\omega_p & -\Omega_p(\exp[i\omega_p t] + \text{c.c.}) & 0 \\ -\Omega_p(\exp[i\omega_p t] + \text{c.c.}) & 2\omega_2 & -\Omega_s(\exp[i\omega_s t] + \text{c.c.}) \\ 0 & -\Omega_s(\exp[i\omega_s t] + \text{c.c.}) & 2\omega_3 \end{pmatrix}, \quad (2.1)$$

where  $\Omega_p$  and  $\Omega_s$  are the time-dependent Rabi frequencies  $\mu\xi_i(t)$  of the pump and Stokes fields, respectively,  $\omega_i$  is the energy of the  $i$ th matter eigenstate, and atomic units are used throughout. After changing to the interaction representation, employing the rotating wave approximation, and specializing to the case of resonant pulses, we obtain [5]

$$\mathbf{H} = -\frac{1}{2} \begin{pmatrix} 0 & \Omega_p & 0 \\ \Omega_p & 0 & \Omega_s \\ 0 & \Omega_s & 0 \end{pmatrix}. \quad (2.2)$$

The eigenstates for this system are displayed in Table I. The now-familiar form of  $|s_2\rangle$  makes possible the counterintuitive excitation scheme in which the Stokes pulse precedes the pump pulse. In this arrangement, all population initially in the ground state projects into  $|s_2\rangle$  ( $\Omega_p \ll \Omega_s$ ), and at the final time all population in  $|s_2\rangle$  projects onto  $|3\rangle$  ( $\Omega_p \gg \Omega_s$ ). This excitation process has been found to be relatively insensitive to the pulse area, and therefore offers near-perfect population transfer to  $|3\rangle$  without the same level of experimental precision demanded by the use of  $\pi$  pulses [14].

### B. Eigenstates of the $V$ system

Before moving on to analyze the properties of four-level systems it is interesting to discuss a second three-level system, depicted in Fig. 1, which consists of two degenerate excited states  $|2\rangle$  and  $|3\rangle$ , and a ground state  $|1\rangle$ . The  $1 \rightarrow 2$  and  $1 \rightarrow 3$  transitions have different transition dipole moments, and thus different Rabi frequencies; however, because they are degenerate, they are excited by the same resonant pulse. Therefore, without loss of generality we may write the Rabi frequencies for the two transitions as  $\beta\Omega$  and  $\gamma\Omega$  such that  $\beta^2 + \gamma^2 = 1$  (see Ref. [5]). Following the same steps that led to Eq. (2.2) we may write the Hamiltonian in the form

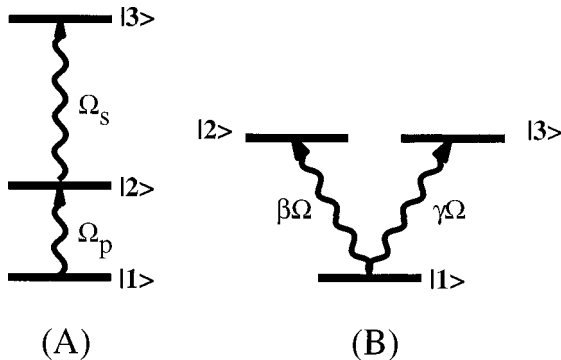


FIG. 1. (a) The three-level ladder configuration described in the text. (b) The three-level  $V$  configuration described in the text.

$$\mathbf{H} = -\frac{1}{2} \begin{pmatrix} 0 & \beta\Omega & \gamma\Omega \\ \beta\Omega & 0 & 0 \\ \gamma\Omega & 0 & 0 \end{pmatrix}. \quad (2.3)$$

The eigenstates of this Hamiltonian are displayed in Table I; they are identical in form to those for the ladder system, with states  $|1\rangle$  and  $|2\rangle$  interchanged. For the  $V$  system,  $|s_2\rangle$  remains unpopulated regardless of the excitation scheme, as the eigenvector has no component on the ground state. The interesting feature of  $|s_2\rangle$  is that the yield in a matter eigenstate varies inversely with its transition dipole moment; the state with the weaker coupling to the ground state is the more heavily populated of the two. While  $|s_2\rangle$  is inaccessible in this system, its existence suggests there may be eigenstates in more complicated systems that are accessible via counterintuitive excitation and that offer opportunities for selective photochemistry.

## III. FOUR-LEVEL BRANCHED SYSTEM

### A. Eigenstates of the four-level system

We turn our attention to the four-level system shown in Fig. 2 with the goal of finding a useful analog to the counterintuitive excitation scheme discussed for the three-level systems in Sec. II. The four-level system consists of a ground state, an intermediate state, and a pair of degenerate product states coupled to the intermediate level by transition dipole moments with different values. This system has been studied by Bergmann and co-workers [5], but they did not specifically address the case where there are degenerate product states. We do so here because, in addition to being the simplest case to treat analytically, selective excitation of

TABLE I. Eigensystems for the three-level systems described in Sec. II.

Label	Ladder configuration	
	Eigenvalues	Eigenvectors
$ s_1\rangle$	$\frac{N_\Omega}{2}$	$(\Omega_p, -\sqrt{\Omega_p^2 + \Omega_s^2}, \Omega_s)/(\sqrt{2}N_\Omega)$
$ s_2\rangle$	0	$(\Omega_s, 0, \Omega_p)/N_\Omega$
$ s_3\rangle$	$-\frac{N_\Omega}{2}$	$(\Omega_p, \sqrt{\Omega_p^2 + \Omega_s^2}, \Omega_s)/(\sqrt{2}N_\Omega)$
		$N_\Omega = \sqrt{\Omega_p^2 + \Omega_s^2}$
		$V$ configuration
$ s_1\rangle$	$\frac{\Omega}{2}$	$(-\Omega, \beta\Omega, \gamma\Omega)/(\sqrt{2}\Omega)$
$ s_2\rangle$	0	$(0, \gamma\Omega, -\beta\Omega)/\Omega$
$ s_3\rangle$	$-\frac{\Omega}{2}$	$(\Omega, \beta\Omega, \gamma\Omega)/(\sqrt{2}\Omega)$

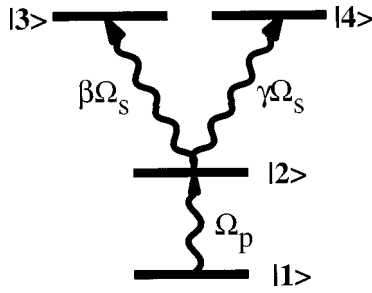


FIG. 2. The four-level system described in the text.

a single state of a degenerate pair represents the most challenging form of control of final-state population.

Performing the same manipulations that were employed in Sec. II we may write the Hamiltonian for the four-level system as

$$\mathbf{H} = -\frac{1}{2} \begin{pmatrix} 0 & \Omega_p & 0 & 0 \\ \Omega_p & 0 & \beta\Omega_s & \gamma\Omega_s \\ 0 & \beta\Omega_s & 0 & 0 \\ 0 & \gamma\Omega_s & 0 & 0 \end{pmatrix}. \quad (3.1)$$

The eigenstates of this Hamiltonian are displayed in Table II. States  $|r_3\rangle$  and  $|r_4\rangle$  are the exact analogs to the states of the three-level system that lead to intuitive excitation. The two degenerate states [17], however, are analogous to a single eigenstate in the three-level system, in that they have a node in the intermediate state. We will explore the behavior of these states in the remainder of this section.

As written,  $|r_1\rangle$  and  $|r_2\rangle$  have a somewhat obscure form. We may simplify the notation by writing

$$\begin{aligned} |r_1\rangle &= \{-\cos[\phi_1] + \cos[\phi_2], 0, \sin[\phi_1], \sin[\phi_2]\}/N_1, \\ |r_2\rangle &= \{-\cos[\phi_1] - \cos[\phi_2], 0, \sin[\phi_1], -\sin[\phi_2]\}/N_2, \\ N_1 &= \sqrt{2}(1 + \cos[\phi_1]\cos[\phi_2])^{1/2}, \\ N_2 &= \sqrt{2}(1 - \cos[\phi_1]\cos[\phi_2])^{1/2}, \end{aligned} \quad (3.2)$$

where

$$\cos[\phi_1] = \frac{\beta\Omega_s}{\sqrt{\Omega_p^2 + \beta^2\Omega_s^2}}, \quad \sin[\phi_1] = \frac{\Omega_p}{\sqrt{\Omega_p^2 + \beta^2\Omega_s^2}},$$

and  $\cos[\phi_2]$  and  $\sin[\phi_2]$  are defined similarly with  $\gamma$  replacing  $\beta$ .

We now make one further notational change in the interests of convenience: Instead of representing  $|r_1\rangle$  and  $|r_2\rangle$  in a vector composed of the bare matter eigenstates  $\{|1\rangle, |2\rangle, |3\rangle, |4\rangle\}$ , we use a vector of the form  $\{|3\rangle, |4\rangle, |1\rangle\}$ , dropping the unnecessary state  $|2\rangle$ . This reordering of the basis states allows us to represent the branching ratio between  $|3\rangle$  and  $|4\rangle$  as the projection of the vector describing the system into the  $XY$  plane of a three-dimensional space. The resultant vectors are

$$|r_1\rangle = \{\sin[\phi_1], \sin[\phi_2], -(\cos[\phi_1] + \cos[\phi_2])\}/N_1,$$

TABLE II. Eigensystem for the discrete four-level system described in Sec. III.

Label	Eigenvalues	Eigenvectors
$ r_1\rangle$	0	$\left\{-\left(\frac{\beta}{N_\beta} + \frac{\gamma}{N_\gamma}\right)\Omega_s, 0, \frac{1}{N_\beta}\Omega_p, \frac{1}{N_\gamma}\Omega_p\right\}/N_1$
$ r_2\rangle$	0	$\left\{-\left(\frac{\beta}{N_\beta} - \frac{\gamma}{N_\gamma}\right)\Omega_s, 0, \frac{1}{N_\beta}\Omega_p, -\frac{1}{N_\gamma}\Omega_p\right\}/N_2$
$ r_3\rangle$	$\frac{N_\Omega}{2}$	$\{\Omega_p, -\sqrt{\Omega_p^2 + \Omega_s^2}, \beta\Omega_s, \gamma\Omega_s\}/(\sqrt{2}N_\Omega)$
$ r_4\rangle$	$-\frac{N_\Omega}{2}$	$\{\Omega_p, \sqrt{\Omega_p^2 + \Omega_s^2}, \beta\Omega_s, \gamma\Omega_s\}/(\sqrt{2}N_\Omega)$

$$N_\Omega = \sqrt{\Omega_p^2 + \Omega_s^2}, \quad N_\beta = \sqrt{\Omega_p^2 + \beta^2\Omega_s^2}, \quad N_\gamma = \sqrt{\Omega_p^2 + \gamma^2\Omega_s^2}$$

$$N_1 = \sqrt{2} \sqrt{1 + \frac{\beta\gamma\Omega_s^2}{N_\beta N_\gamma}}, \quad N_2 = \sqrt{2} \sqrt{1 - \frac{\beta\gamma\Omega_s^2}{N_\beta N_\gamma}}$$

$$|r_2\rangle = \{\sin[\phi_1], -\sin[\phi_2], -(\cos[\phi_1] - \cos[\phi_2])\}/N_2. \quad (3.3)$$

The notation introduced here is convenient, because if one excites the system with a pair of pulses in the counterintuitive configuration both  $\phi_1$  and  $\phi_2$  go from 0 to  $\pi/2$ . During excitation,  $|r_1\rangle$  begins as a vector on the  $Z$  axis and rotates into the  $XY$  plane, whereas  $|r_2\rangle$  begins and ends in the  $XY$  plane and has no component along the  $Z$  axis at short times. Thus, all of the ground-state population is initially in  $|r_1\rangle$ ; in the absence of nonadiabatic coupling this initial condition leads, after excitation ( $\lim_{\Omega_s \rightarrow 0} \sin[\phi_1] = \lim_{\Omega_s \rightarrow 0} \sin[\phi_2] = 1$ ), to equal populations in the matter states  $|3\rangle$  and  $|4\rangle$ . However,  $|r_1\rangle$  and  $|r_2\rangle$  are degenerate, and nonadiabatic coupling between them must be taken into account.

### B. Nonadiabatic effects

If the eigenstates of a system are given by  $|g_i\rangle$  and have energy  $\epsilon_i$ , the wave function  $|\Psi\rangle$  for the system may be written as

$$|\Psi\rangle = \sum_k \alpha_k \exp\left[-i \int_{-\infty}^t d\tau g_k\right] |g_k\rangle, \quad (3.4)$$

where  $g_k = \epsilon_k - i\langle g_k | \dot{g}_k \rangle$ , with  $|\dot{g}_k\rangle$  denoting the time derivative of  $|g_k\rangle$ . The coefficients  $\alpha_k$  then obey the equation [5,16]

$$\dot{\alpha}_k = -\sum_{i \neq k} \alpha_i \langle g_k | \dot{g}_i \rangle \exp\left[i \int_{-\infty}^t d\tau (g_k - g_i)\right]. \quad (3.5)$$

If  $|\epsilon_k - \epsilon_i| \gg \langle g_k | \dot{g}_i \rangle$ , the system will evolve adiabatically. We are therefore justified in neglecting the possibility of nonadiabatic coupling to  $|r_3\rangle$  and  $|r_4\rangle$ , as these states have nonzero eigenvalues.  $|r_1\rangle$  and  $|r_2\rangle$  are degenerate, however, and we must take their coupling into account.

The relevant quantities for the present case are

$$k_c = \langle r_1 | \dot{r}_2 \rangle = -\langle r_2 | \dot{r}_1 \rangle$$

TABLE III. Absolute and relative yields for simulations of a four-level system.

$\beta^2$	Absolute yield	Relative yield
	$\langle\langle 3 3\rangle + \langle 4 4\rangle\rangle$	$\frac{\langle 3 3\rangle}{\langle\langle 3 3\rangle + \langle 4 4\rangle\rangle}$
0.500 000 00	0.999 844 09	0.500 000 00
0.490 000 00	0.999 844 09	0.490 000 00
0.400 000 00	0.999 844 09	0.400 000 00
0.100 000 00	0.999 844 09	0.100 000 00
0.010 000 00	0.999 844 09	0.010 000 00
0.001 000 00	0.999 844 09	0.001 000 00

$$= \frac{(\dot{\phi}_2 \sin[\phi_2] \cos[\phi_1] - \dot{\phi}_1 \sin[\phi_1] \cos[\phi_2])}{2(1 - \cos[\phi_1]^2 \cos[\phi_2]^2)^{1/2}},$$

$$\langle r_1 | \dot{r}_1 \rangle = \langle r_2 | \dot{r}_2 \rangle = 0,$$

$$r_1 = \epsilon_1 - i \langle r_1 | \dot{r}_1 \rangle = 0; \quad r_2 = \epsilon_2 - i \langle r_2 | \dot{r}_2 \rangle = 0. \quad (3.6)$$

When Eq. (3.6) is combined with Eq. (3.5) we obtain the coupled differential equations

$$\begin{aligned} \dot{\alpha}_1 &= -k_c \alpha_2, \\ \dot{\alpha}_2 &= -k_c \alpha_1. \end{aligned} \quad (3.7)$$

When the Stokes pulse precedes the pump pulse the initial conditions for Eq. (3.7) are

$$\begin{aligned} \alpha_1(t=0) &= 1, \\ \alpha_2(t=0) &= 0. \end{aligned} \quad (3.8)$$

One trivial case presents itself immediately: If  $\beta^2 = \gamma^2 = \frac{1}{2}$ , then  $k_c = 0$  and there is no population transfer between  $|r_1\rangle$  and  $|r_2\rangle$ . Thus, in this case, at the final time the populations of the matter eigenstates  $|3\rangle$  and  $|4\rangle$  are equal. For more general cases we must examine the results of simulations.

### C. Numerical results

We look first at how the relative populations in  $|3\rangle$  and  $|4\rangle$  vary with the transition dipole moment. The results of a series of simulations using identical pulse parameters but varying  $\beta$  and  $\gamma$  are shown in Table III. As can be anticipated from the forms of  $|r_1\rangle$  and  $|r_2\rangle$ , the total yield in the product states is found to be near unity for the pulse parameters employed, and is independent of the individual transition dipole moments  $\beta$  and  $\gamma$ . We note that, to within the accuracy of the simulation, the relative population in  $|3\rangle$  is always exactly the square of the relative transition dipole moment  $\beta^2$ . This is possible only through a superposition of  $|r_1\rangle$  and  $|r_2\rangle$ , and it is clear that nonadiabatic coupling acts to provide exactly the same ratio of population as the transition dipole moments do in intuitive excitation. Further simulations [18] show that this is true regardless of pulse area or overlap.

The origin of this effect lies in the form of  $k_c$ . The time derivative of the field does not appear explicitly in the for-

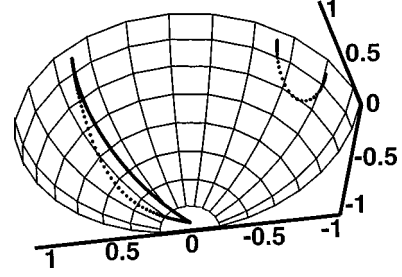


FIG. 3. Time evolution of the eigenvectors  $|r_1\rangle$  and  $|r_2\rangle$  for  $\beta^2 = \gamma^2$  (solid) and  $\beta^2 = 0.1$ ,  $\gamma^2 = 0.9$  (dotted). The eigenvectors inscribe arcs on the surface of a unit sphere; see text for details.

mula, but rather is contained in the form of the time derivatives  $\dot{\phi}_1$  and  $\dot{\phi}_2$ . Since  $\phi_1$  and  $\phi_2$  are determined solely by the relative magnitudes of the two fields, any scheme in which  $\phi_1$  and  $\phi_2$  go from 0 to  $\pi/2$  will give the same yield for a given  $\beta$  and  $\gamma$ . Figure 3 shows graphically the path taken by the eigenvectors as they evolve; for the case where  $\gamma = \beta$ ,  $|r_2\rangle$  is fixed with respect to time and  $|r_1\rangle$  traces an arc along the  $45^\circ$  line in the first quadrant of the  $\mathbf{34}$  plane. At all times the vector  $|\dot{r}_1\rangle$  describing the ‘‘velocity’’ of the  $|r_1\rangle$  eigenstate is perpendicular to  $|r_2\rangle$ , and  $\langle r_2 | \dot{r}_1 \rangle = \langle r_1 | \dot{r}_2 \rangle = 0$ . This is the geometric consequence of the observation that if  $\beta = \gamma$ ,  $k_c = 0$ .

The situation is more interesting when  $\beta \neq \gamma$ , as shown in Fig. 3. In this case the  $|r_2\rangle$  vector evolves, beginning at an angle  $\chi = \arctan[\beta/\gamma]$  in the fourth quadrant of the  $\mathbf{34}$  plane, swinging out of the plane and then returning at  $\chi = 45^\circ$ . The projection of  $|r_1\rangle$  in the  $\mathbf{34}$  plane begins and ends at a  $45^\circ$  angle in the first quadrant, but deviates from the  $45^\circ$  path at intermediate times. In this case,  $\langle r_2 | \dot{r}_1 \rangle = \langle r_1 | \dot{r}_2 \rangle \neq 0$  and it is clear that the value of  $k_c$  is determined by the change in geometry rather than the change in time *per se*. Further,  $k_c$  is linear in  $\dot{\phi}_1$  and  $\dot{\phi}_2$ , so while altering the envelope of the field may cause  $|r_1\rangle$  and  $|r_2\rangle$  to oscillate, there will be no change in the net population transfer at the final time. Thus, while the nature of the nonadiabatic population transfer between  $|r_2\rangle$  and  $|r_1\rangle$  is by no means obvious, the geometric representation of the process does shed some light on the stability of population transfer with respect to changes in the field.

The four-level system studied here seems to offer no method with which to target either degenerate state in counterintuitive excitation; the ratio of populations in each of the target states is dependent solely on transition dipole moments and is beyond experimental control. In the next section, however, we will show that the addition of coupling to a fifth state by a third laser changes the situation dramatically and creates intriguing new possibilities for selective photochemistry.

## IV. FIVE-LEVEL BRANCHED SYSTEM

### A. Eigenstates of the five-level system

Given that variation of the existing laser fields  $\Omega_p$  and  $\Omega_s$  seems to have no effect on the relative populations in the degenerate target states, it is natural to consider using a third pulse to extend the system via coupling to a fifth state. Ac-

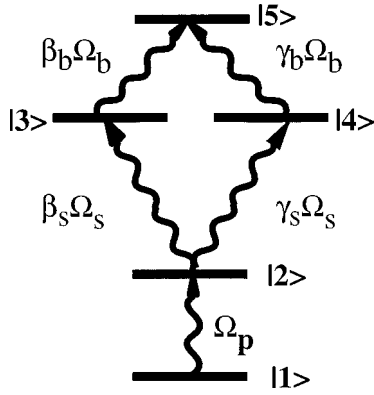


FIG. 4. The five-level system described in the text.

cordingly, we now consider the consequences of adding a third laser, referred to as the “branch” laser, which couples the degenerate target states to a fifth level as shown in Fig. 4. The only restriction on the choice of  $|5\rangle$  is that the frequency of the branch transition must not be resonant with either the pump or the Stokes transitions. We use the same  $\beta$ ,  $\gamma$  notation to treat the branch transition as we do the Stokes transition, and write the Hamiltonian in the form

$$\mathbf{H} = -\frac{1}{2} \begin{pmatrix} 0 & \Omega_p & 0 & 0 & 0 \\ \Omega_p & 0 & \beta_s \Omega_s & \gamma_s \Omega_s & 0 \\ 0 & \beta_s \Omega_s & 0 & 0 & \beta_b \Omega_b \\ 0 & \gamma_s \Omega_s & 0 & 0 & \gamma_b \Omega_b \\ 0 & 0 & \beta_b \Omega_b & \gamma_b \Omega_b & 0 \end{pmatrix}. \quad (4.1)$$

The eigenvalues of Eq. (4.1) are displayed in Table IV; the eigenvectors are cumbersome in form, and we do not tabulate them here. It is sufficient to note that in the limit  $\Omega_p \rightarrow 0$  only the null eigenvector has a nonzero projection in the ground state; thus, as in the three- and four-level cases, only the null eigenvector will be populated by an excitation scheme in which the Stokes pulse precedes the pump pulse.

The forms of the eigenvalues make it apparent that we should expect behavior that is significantly different from that observed in the four-level system. Population transfer in the four-level system is dominated by nonadiabatic coupling between a pair of degenerate dressed eigenstates; here, no

TABLE IV. Eigenvalues of a five-level system.  $N_{\text{tot}} = \sqrt{\Omega_p^2 + \Omega_s^2 + \Omega_b^2}$ .

$(-\sqrt{N_{\text{tot}}^2 + \sqrt{N_{\text{tot}}^4 - 4\{\Omega_p^2 + [\gamma_s^2 + \gamma_b^2 - 2\gamma_s\gamma_b(\gamma_s\gamma_b + \beta_s\beta_b)]\Omega_s^2\}\Omega_b^2})/2\sqrt{2}$
$(-\sqrt{N_{\text{tot}}^2 - \sqrt{N_{\text{tot}}^4 - 4\{\Omega_p^2 + [\gamma_s^2 + \gamma_b^2 - 2\gamma_s\gamma_b(\gamma_s\gamma_b + \beta_s\beta_b)]\Omega_s^2\}\Omega_b^2})/2\sqrt{2}$
0
$(\sqrt{N_{\text{tot}}^2 - \sqrt{N_{\text{tot}}^4 - 4\{\Omega_p^2 + [\gamma_s^2 + \gamma_b^2 - 2\gamma_s\gamma_b(\gamma_s\gamma_b + \beta_s\beta_b)]\Omega_s^2\}\Omega_b^2})/2\sqrt{2}$
$(\sqrt{N_{\text{tot}}^2 + \sqrt{N_{\text{tot}}^4 - 4\{\Omega_p^2 + [\gamma_s^2 + \gamma_b^2 - 2\gamma_s\gamma_b(\gamma_s\gamma_b + \beta_s\beta_b)]\Omega_s^2\}\Omega_b^2})/2\sqrt{2}$

such degeneracy exists and the adiabatic approximation will hold. The null eigenvector is given by

$$|r_0\rangle = \{-(\beta_b\gamma_s - \gamma_b\beta_s)\Omega_s, 0, -\gamma_b\Omega_p, \beta_b\Omega_p, 0\}/N_b, \quad (4.2)$$

where  $N_b = \sqrt{\Omega_p^2 + (\beta_s\gamma_b - \gamma_s\beta_b)^2\Omega_s^2}$ . Note that while  $\Omega_b$  does not appear explicitly in the eigenvector, the third field must be present for the duration of both the pump and Stokes fields for the eigenstate to exist. Physically, this means it must either be a long pulse overlapping both fields or a continuous wave field.

For our purposes, namely, selective population of a degenerate state,  $|r_0\rangle$  represents a potentially useful eigenstate. First, it has nodes in  $|2\rangle$  and  $|5\rangle$ , indicating that in counterintuitive excitation 100% of the population will be transferred to the degenerate target states. Second, the branching ratio between those states is determined entirely by the coupling to  $|5\rangle$ , which may be chosen arbitrarily from almost any of the available states of the system. And, finally, the relative populations of the degenerate states are reversed with respect to their respective transition strengths for the  $\{|3\rangle, |4\rangle\} \rightarrow |5\rangle$  transitions.

To illustrate the implications of this observation, consider a case in which  $|5\rangle$  is chosen such that the  $|3\rangle \rightarrow |5\rangle$  transition is symmetry forbidden. In this limit,  $\beta_b = 0$  and  $\gamma_b = 1$ , so that the eigenstate becomes

$$|r_0\rangle = \{\beta_s\Omega_s, 0, -\Omega_p, 0, 0\}/N_b \quad (4.3)$$

and 100% of the population is transferred to  $|3\rangle$ . Thus, if a convenient branch state exists in the system it is possible to achieve near-perfect control over both relative and absolute populations of a pair of degenerate states.

There is a less useful limit that we will also consider. The form of Eq. (4.2) implies that if  $(\beta_b\gamma_s - \gamma_b\beta_s) = 0$  (i.e., if  $\beta_s = \beta_b$ ), there is a node in the ground state and  $|r_0\rangle$  will remain unpopulated even in counterintuitive excitation. In the next section we will show that both this limit and that given in Eq. (4.3) may be explained with reference to the symmetry of the system.

## B. Symmetry of the Hamiltonian

Clearly, there is an important difference in the nature of population transfer in the four- and five-level systems described here. Under counterintuitive excitation population transfer in the four-level system is dominated by two zero-energy eigenvectors, one of which is directly populated on excitation and the other of which is populated via nonadiabatic coupling. The five-level system contains only one null eigenvector, which may or may not be populated on excitation from the ground state depending on the nature of the fifth state.

The origin of this change in behavior lies in the symmetry of the Hamiltonian. To illustrate the symmetry we refer to the special case where all nonzero elements of the Hamiltonian are equal, a situation that is not possible for the duration of the excitation process but that may be achieved at intermediate times. For the Hamiltonian given in Eq. (3.1) this means setting  $\beta = \gamma$ ,  $\Omega_s = \Omega_p/\sqrt{2}$ , and writing

$$\mathbf{H} = -\frac{\Omega_p}{2} \begin{pmatrix} 0 & 1 & 0 & 0 \\ 1 & 0 & 1 & 1 \\ 0 & 1 & 0 & 0 \\ 0 & 1 & 0 & 0 \end{pmatrix}. \quad (4.4)$$

In this limit we may use elementary linear algebra to obtain the symmetry of the matrix [19]. The Hamiltonian given above is invariant under the exchange of states  $|1\rangle$ ,  $|3\rangle$ , and  $|4\rangle$ ; we may think of this as a threefold symmetry around an ‘‘axis’’ defined by  $|2\rangle$ . Ignoring the relative phases of the components of the eigenstates, we may say that  $|r_1\rangle$  corresponds to a threefold symmetry about  $|2\rangle$ , and  $|r_2\rangle$  corresponds to a twofold symmetry about an axis containing states  $|1\rangle$  and  $|2\rangle$ . The hypothetical axes discussed here are significant not simply with respect to the exchange of states but also for the presence of nodes in the matter eigenstates along those axes in the dressed eigenstates.

Let us apply these ideas to the case of the five-level system, and take the limit in which pump and Stokes parameters are treated as above, and  $\gamma_b = 1$ ,  $\beta_b = 0$ , and  $\Omega_b = \Omega_p$ . This yields the equation

$$\mathbf{H} = -\frac{\Omega_p}{2} \begin{pmatrix} 0 & 1 & 0 & 0 & 0 \\ 1 & 0 & 1 & 1 & 0 \\ 0 & 1 & 0 & 0 & 0 \\ 0 & 1 & 0 & 0 & 1 \\ 0 & 0 & 0 & 1 & 0 \end{pmatrix}. \quad (4.5)$$

The existence of the fifth state breaks the symmetry, leaving the Hamiltonian invariant only for the exchange of states  $|1\rangle$  and  $|3\rangle$ , a twofold symmetry. This gives rise to a single null eigenvector with nodes in states  $|2\rangle$ ,  $|4\rangle$ , and  $|5\rangle$ . Taking the opposite limit, such that  $\gamma_b = \beta_b$ ,  $\Omega_b = \Omega_p/\sqrt{2}$ , the equation becomes

$$\mathbf{H} = -\frac{\Omega_p}{2} \begin{pmatrix} 0 & 1 & 0 & 0 & 0 \\ 1 & 0 & 1 & 1 & 0 \\ 0 & 1 & 0 & 0 & 1 \\ 0 & 1 & 0 & 0 & 1 \\ 0 & 0 & 1 & 1 & 0 \end{pmatrix}. \quad (4.6)$$

Now the twofold axis of symmetry lies in states  $|1\rangle$ ,  $|2\rangle$ , and  $|5\rangle$ , and the resultant dressed eigenstate includes a node on the ground state that makes counterintuitive population transfer to the target states impossible. The role of the fifth state is therefore to break the symmetry of the four-level system, eliminating one null eigenvector and shifting the axis of symmetry. The symmetries of all three systems are depicted schematically in Fig. 5. The qualitative argument presented here is not intended to provide detailed insight into the nature of the process, but rather to raise the possibility that there might be an underlying group theory for such branched systems which is similar to the  $SU(N)$  group theory used to evaluate ladder systems [20].

The results of a series of simulations are given in Tables V and VI. As we would expect from the form of  $|r_0\rangle$ , the relative yield in state  $|3\rangle$  is determined by the  $4 \rightarrow 5$  coupling

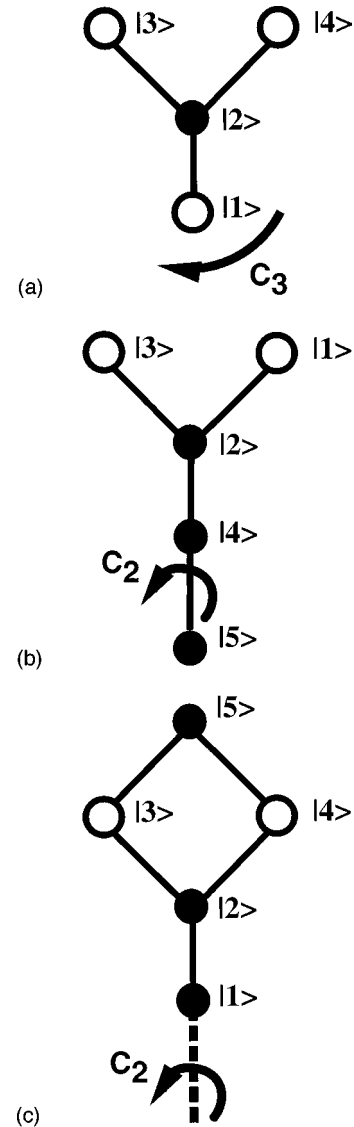


FIG. 5. Schematic diagrams showing the symmetry of the systems; open circles represent matter eigenstates possessing nonzero components of the dressed eigenvector, while states that are nodes are designated by solid circles. (a) The four-level system (threefold symmetry); (b) the five-level system in the limit where the  $|3\rangle \rightarrow |5\rangle$  transition is forbidden; (c) the five-level system in the limit where  $(\beta_b \gamma_s - \gamma_b \beta_s) = 0$ .

term  $\gamma_b$ . The absolute yield varies as expected, staying near unity except in the limit where  $\beta_s \rightarrow \beta_b$ . The procedure is robust in that the yield does not vary significantly from unity until  $|\beta_s^2 - \beta_b^2| < 1\%$ , indicating that this limitation on the method is unlikely to be important except in the most pathological of cases.

### C. Practical considerations

When evaluating the applicability of the methods described here, it is useful to review what is known for the case of StiRAP in three-level systems. Despite the successful experimental implementation of StiRAP in atomic [11,12] and molecular [10] systems, many questions remain concerning the applicability of adiabatic passage excitation in physically realistic systems. One issue is whether adiabatic passage is

TABLE V. Parameters for calculations for four- and five-level systems. The Schrödinger equation was numerically integrated using a Lanczos propagator in an atomic basis.

		System		
$E_1=0$	$E_2=10\text{ cm}^{-1}$		$E_{3,4}=110\text{ cm}^{-1}$	$E_5=155\text{ cm}^{-1}$
		Field		
Pulse	$t_{\text{max}}$ (ns)	FWHM (ns)	$\omega$ ( $\text{cm}^{-1}$ )	$\Omega_{\text{max}}$ (THz) <sup>a</sup>
Pump	6	12	100	0.4,4
Stokes	-6	12	10	0.4,4
Branch	0	$\infty^b$	45	0,4

<sup>a</sup>The first number pertains to simulations in the four-level system, the second to the five-level system.

<sup>b</sup>The branch field was taken to be time independent.

possible in cases where the laser field may couple additional states to the system, destroying the symmetry necessary to maintain the counterintuitively accessed eigenstate. While such couplings may lead to some lessening of population transfer, it has been shown that one may maintain an extremely high yield even in the presence of coupling to discrete states [5]. Numerical simulations suggest that the same is true for at least some cases involving coupling to the continuum, though the situation is much more complicated [15]. Obviously researchers must choose excitation pathways carefully to avoid additional resonant transitions and minimize such couplings, but a high level of population transfer is possible even in the presence of such processes.

Another concern is the possibility of decay from the states involved in the process. Such decay could result from either radiative or radiationless transitions to states not included in the calculation, or from losses to continuum states. The question of whether adiabatic passage is possible in systems including resonant or even continuum states has been the subject of much debate in the literature [21–24], and it is known that the criteria for adiabaticity break down in the presence of decays [16]. However, if the Rabi frequencies for the transition are sufficiently large relative to the rate of decay, nonadiabatic effects are minimal and near-perfect population transfer remains possible. Thus, given sufficiently intense fields, a close approximation to adiabatic passage is possible in three-level systems.

These problems are not yet firmly resolved even for three-level systems, however, and a detailed treatment incorporating four- and five-level systems as well would be even more demanding. We wish to note that just as the state  $|s_2\rangle$  given in Table I remains an eigenvector of the three-level system even in the presence of a decaying intermediate state [16],

TABLE VI. Results from calculations on a five-level system, with  $\beta_s^2 = \gamma_s^2 = 0.5$ .

$\gamma_b^2$	Absolute yield in $ 3\rangle$ and $ 4\rangle$	Relative yield in $ 3\rangle$
1.000 000	1.000 000	1.000 000
0.750 000	0.750 000	0.750 000
0.600 000	0.999 997	0.600 000
0.550 000	0.999 981	0.550 000
0.510 000	0.994 144	0.510 000
0.505 000	0.771 684	0.505 000
0.500 000	$3.9 \times 10^{-8}$	0.500 000

the eigenstate  $|r_0\rangle$  [Eq. (4.2)] of the five-level system remains an eigenstate even in the presence of a decaying branch state, as in a Hamiltonian of the form

$$\mathbf{H} = -\frac{1}{2} \begin{pmatrix} 0 & \Omega_p & 0 & 0 & 0 \\ \Omega_p & 0 & \beta_s \Omega_s & \gamma_s \Omega_s & 0 \\ 0 & \beta_s \Omega_s & 0 & 0 & \beta_b \Omega_b \\ 0 & \gamma_s \Omega_s & 0 & 0 & \gamma_b \Omega_b \\ 0 & 0 & \beta_b \Omega_b & \gamma_b \Omega_b & i\Gamma \end{pmatrix}. \quad (4.7)$$

We therefore expect qualitatively similar behavior with respect to decay, such that either the intermediate or branch states of the five-level system may be resonances or continua, provided the laser fields are sufficiently intense to force near-adiabatic behavior. Simulations suggest the same is true for the target states of the five-level system, but that work is still in progress [28].

The next logical question is how one may construct four- and five-level systems of this type within physical systems. We must first identify two degenerate target states corresponding to the desired chemical products, then find an intermediate state that will couple them to the ground state and a branch state with the desired transition dipole moments. It is important to remember that the relative energies of the states are irrelevant to adiabatic passage. For resonant pulses, the form of the Hamiltonian in Eq. (4.1) is independent of whether the matter eigenstate energy  $E_i > E_j$  for any  $i$  and  $j$  in the system; for nonresonant pulses, the difference is purely in the sign of the phase. The symmetries described above depend not on the energy, which is implicitly contained in the choice of laser frequency, but on the morphology of the system deriving from the transition dipole moments.

With these general principles in mind, we now examine in detail how one might apply this control technique to a real molecular system. For purposes of discussion, we choose HNCO, a molecule that has been studied extensively in the context of control of formation of photochemical products [25–27]. The system is known to photodissociate on excitation above  $\sim 240$  nm, and Crim and co-workers [25,26] have shown that two pathways become available at these energies:  $\text{HNCO} \rightarrow \text{H} + \text{NCO}$  and  $\text{HN} + \text{CO}$ , both shown schematically in Fig. 6. These researchers have further discovered that while cleavage of the NC bond is heavily favored

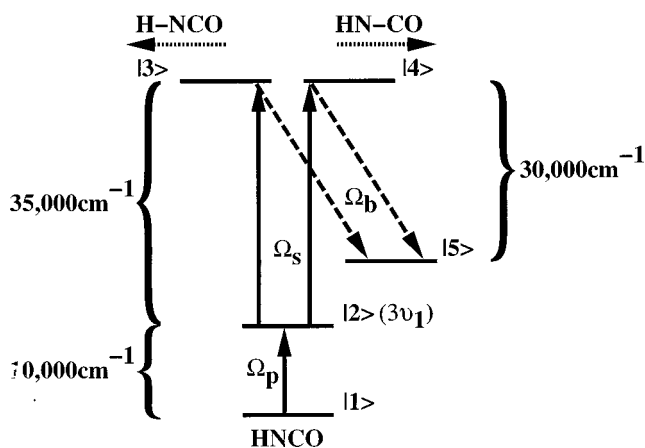


FIG. 6. The HNCO system described in the text.

for single-photon excitation at 225 nm, the situation changes for resonantly enhanced two-photon excitation. If two lasers are tuned so that the  $3\nu_1$  state (corresponding to three quanta in the N-H stretch) serves as a resonant intermediate state, N-H cleavage becomes the favored pathway for photodissociation.

It is known that the mechanism for N-H bond cleavage at that energy involves the decay of a resonant state with a lifetime on the order of 2 ps [26]. It is not known if a similar state exists for C-N cleavage, but for purposes of discussion we will assume that this is the case. We may now view the molecule as a four-level system consisting of a ground state, an intermediate state, and a pair of degenerate target states; the latter may not be strictly degenerate, but if the density of states is large compared to the width of the resonance or the bandwidth of the pulses the behavior should be qualitatively similar to that of the degenerate case. The fact that the target states are narrow resonances complicates the situation, but as discussed above StiRAP-like processes should still be possible [15,16]. There has also been some experimental work on subpicosecond StiRAP-like excitation [12] that implies that the relevant time scale is experimentally accessible. Within this context, the four-level system may be viewed as having a Hamiltonian of the form given in Eq. (3.1).

Let us assume that we wish to selectively cleave the N-H bond at this energy using a process which will maximize the absolute yield in this channel. While a single-photon excitation will provide better than 80% relative yield in the H+NCO channel [26], the  $\pi$  pulse necessary for complete population transfer is experimentally less robust than a StiRAP-like two-photon process. The two-photon scheme described in Sec. III here provides only a 20% relative yield in the desired channel, so while complete population transfer to the degenerate states is possible in the strong-field limit, the relative yield is not very good. Choosing a different intermediate level is awkward in this case, as the 225-nm region lies  $\sim 5000\text{ cm}^{-1}$  above the origin of the excited electronic state. An intermediate level that is less than  $5000\text{ cm}^{-1}$  above the ground state, then, will lead to a situation in which the Stokes laser has sufficient energy to couple the ground state to states in the low-energy tail of the excited electronic manifold. The  $3\nu_1$  level represents a good intermediate state because it lies  $\sim 10\,000\text{ cm}^{-1}$  above the ground vibrational state, and the highly anharmonic nature of

the N-H stretch makes its overtones directly accessible from the ground state.

This problem may be overcome with the use of a fifth state, coupled to the degenerate target states with a branch laser, as shown in Fig. 6. Based on the form of the null eigenvector in Eq. (4.2), if we desire to enhance the yield in the C-N cleavage pathway (produced by dissociation from state |4>) we must choose a fifth state that couples preferentially to the state leading to the N-H cleavage pathway |3>. The choice of the fifth state is also dictated by the energetics of the other states of the system; the branch laser must not be resonant with any significant transition from the ground state, nor should it be resonant for any transition from the intermediate state |2). |5) should therefore lie at least  $5000\text{ cm}^{-1}$  above the energy of state |2), so that the |3)  $\rightarrow$  |5) transition has sufficiently low energy to avoid coupling |2) to the excited electronic state.

There is at present very limited information on the vibrational states of HNCO at the energies cited above. Most states in the energy range of interest are inaccessible from the ground state by Raman transitions [26], though the  $\nu_1$  progression is strong enough that it has been populated by direct absorption from the ground state as high as the  $4\nu_1$  overtone, which lies roughly  $13\,200\text{ cm}^{-1}$  above the ground state. The  $4\nu_1$  overtone is, like the  $3\nu_1$  state, known to have a strong overlap with the region of the excited state of interest.

The  $4\nu_1$  overtone is only  $\sim 3000\text{ cm}^{-1}$  above the  $3\nu_1$  ( $|2\rangle$ ) state, and a laser that couples it to the target states therefore opens an undesirable route of excitation from |2). The fifth overtone, however, may serve our purpose; it should be sufficiently high in energy, and should have the same favorable overlaps with the N-H dissociative channel as the  $3\nu_1$  overtone. The  $5\nu_1$  state has never been observed, having too small a transition moment coupling with the ground state; the issue here, however, is its transition strength with the excited state, and the trend of transition strengths in the third and fourth overtones suggests it should be sufficient for our purposes.

While we do not have the detailed knowledge of energies or coupling strengths necessary to carry out a calculation of the expected enhancement of yield of the product, this example should serve to illustrate the factors involved in constructing a controlled dissociation pathway of the desired form. In this case, the states |2) and |5) are part of the same progression, and (we assume) have qualitatively similar relative transition dipole moments; use of the technique outlined here thus represents a reversal of the qualitative trend belonging to that family of states. This represents a powerful form of control, allowing researchers to selectively populate a given state *because* it is accessed via an unfavorable transition in conventional excitation.

After completion of the work described in this paper we became aware of some striking similarities between the theory presented here and the simulations of photoexcitation of the sodium dimer carried out by Shapiro, Chen, and Brumer [29]. These investigators couple a set of three discrete states to the continuum, and monitor dissociation along two isoenergetic paths in the continuum:  $\text{Na}_2 \rightarrow \text{Na}(3s) + \text{Na}(3p)$  and  $\text{Na}(3s) + \text{Na}(3d)$ . Where the configuration of



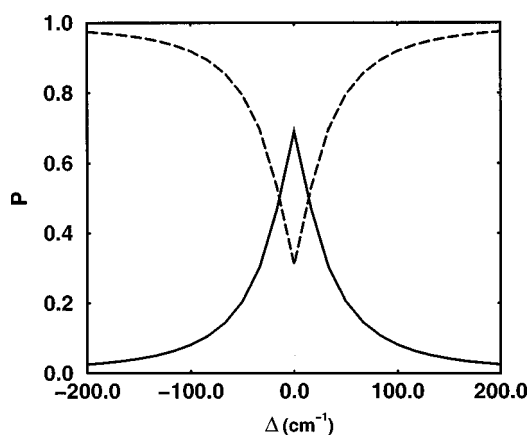


FIG. 7. Results of simulations of the sodium dimer, based on the model of Shapiro, Chen, and Brumer. Solid: Yield in the Na( $3d$ ) channel. Dashed: Yield in the Na( $3p$ ) channel. The relative transition dipole moments are given by  $\beta_s^2 < 1\%$ ,  $\gamma_s^2 > 99\%$ ;  $\beta_b^2 = 69\%$ ,  $\gamma_b^2 = 31\%$ , where  $\beta$  and  $\gamma$  correspond to couplings with the  $3d$  and  $3p$  channels, respectively.

the electric fields matches that of the scheme reported here, the results are consistent with the predictions of our theory.

While the details of the calculation will be the subject of a future paper [28], we have included the results of one sample calculation in this work. The results of the simulation are shown in Fig. 7, where the yield in each channel is plotted as a function of the detuning of the branch laser. One expects that in the limit of large detuning, the system will behave as a four-level system, while when the transition is near resonance it behaves as a five-level system. The results shown in Fig. 7 are consistent with this view. The most

interesting feature of the sodium case is the fact that the target states are dissociative, leading to a decay term that prevents truly adiabatic passage. The results of simulations such as those included in Fig. 7 indicate that adiabatic passage-based control is still possible in the presence of dissociative states. However, their existence affects the process in complicated ways and we defer discussion of such effects for future work where they may be treated in greater detail.

## V. CONCLUSIONS

In this paper, we have extended existing work on counterintuitively ordered two-pulse laser-induced population transfer to systems with multiple target states. We have found that while the simplest possible four-level system may not be selectively populated by two counterintuitively ordered pulses, the addition of a third field coupling the target state to a fifth state breaks the symmetry of the four-level system and makes selective excitation possible. Selectivity is based on the coupling strength of the fifth level to the degenerate target states, and the fifth level must be chosen to have appropriate properties for the desired effect. The challenge in this form of control is therefore not in the determination of an optimal electric field *per se*, but rather in the construction of a photosensitive pathway from the available states of the system.

## ACKNOWLEDGMENT

This research was supported by a grant from the National Science Foundation (No. CHE 9216073).

- 
- [1] U. Gaubatz, P. Rudecki, S. Schiemann, and K. Bergmann, *J. Chem. Phys.* **92**, 5363 (1990).
- [2] B. W. Shore, K. Bergmann, J. Oreg, and S. Rosenwaks, *Phys. Rev. A* **44**, 7442 (1991).
- [3] V. S. Malinovsky and D. J. Tannor, *Phys. Rev. A* **56**, 4929 (1997).
- [4] J. Oreg, K. Bergmann, B. W. Shore, and S. Rosenwaks, *Phys. Rev. A* **45**, 4888 (1992).
- [5] G. W. Coulston and K. Bergmann, *J. Chem. Phys.* **96**, 3467 (1992).
- [6] B. W. Shore, J. Martin, M. P. Fewell, and K. Bergmann, *Phys. Rev. A* **52**, 566 (1995); J. Martin, B. W. Shore, and K. Bergmann, *ibid.* **52**, 583 (1995).
- [7] For a review, see K. Bergmann and B. W. Shore, *Molecular Dynamics and Spectroscopy by Stimulated Emission Pumping*, edited by H. C. Dai and R. W. Field (World Scientific, Singapore, 1995).
- [8] Y. B. Band and O. Magnes, *J. Chem. Phys.* **101**, 7528 (1994).
- [9] Y. B. Band, *Phys. Rev. A* **50**, 584 (1994); Y. B. Band and O. Magnes, *ibid.* **50**, 5046 (1994).
- [10] T. Halfmann and K. Bergmann, *J. Chem. Phys.* **104**, 7068 (1996); S. Schiemann, A. Kuhn, S. Steuerwald, and K. Bergmann, *Phys. Rev. Lett.* **71**, 3637 (1993); **69**, 2062 (1992).
- [11] J. Martin, B. W. Shore, and K. Bergmann, *Phys. Rev. A* **54**, 1556 (1996).
- [12] B. Broers, H. B. van Linden van den Heuvell, and L. D. Noordam, *Phys. Rev. Lett.* **69**, 2062 (1992).
- [13] For reviews, see W. S. Warren, H. Rabitz, and M. Dahleh, *Science* **259**, 1581 (1993); S. A. Rice, *Adv. Chem. Phys.* **101**, 213 (1997).
- [14] M. D. Levenson and S. S. Kano, *Introduction to Nonlinear Laser Spectroscopy*, 2nd ed. (Academic, New York, 1988).
- [15] T. Nakajima and P. Lambropoulos, *Z. Phys. D* **36**, 17 (1996).
- [16] M. N. Kobrak and S. A. Rice, *Phys. Rev. A* **57**, 1158 (1998).
- [17] These states are identical to those given in [5], but we express them using a different linear combination of the eigenvectors to emphasize symmetries brought about by the degeneracy of the final states.
- [18] M. N. Kobrak and S. A. Rice (unpublished).
- [19] F. A. Cotton, *Chemical Applications of Group Theory*, 3rd ed. (Wiley and Sons, New York, 1990).
- [20] F. T. Hioe and J. H. Eberly, *Phys. Rev. Lett.* **47**, 838 (1981).
- [21] T. Nakajima, M. Elk, J. Zhang, and P. Lambropoulos, *Phys. Rev.* **50**, 913 (1994).
- [22] B. Dai and P. Lambropoulos, *Phys. Rev. A* **36**, 5205 (1987).
- [23] C. E. Carroll and F. T. Hioe, *Phys. Rev. Lett.* **68**, 3523 (1992); C. E. Carroll and F. T. Hioe, *Phys. Lett. A* **199**, 145 (1995).
- [24] N. V. Vitanov and S. Stenholm, *Phys. Rev. A* **56**, 741 (1997).
- [25] S. S. Brown, R. B. Metz, H. L. Berghout, and F. F. Crim, *J.*

- Chem. Phys. **105**, 6293 (1996); S. S. Brown, C. M. Cheatum, D. A. Fitzwater and F. F. Crim, *ibid.* **105**, 10 911 (1996).
- [26] S. S. Brown, Doctoral thesis (University of Wisconsin at Madison, Wisconsin, 1996).
- [27] M. Zyrianov, Th. Droz-Georget, A. Sanov, and H. Reisler, J. Chem. Phys. **105**, 8111 (1996).
- [28] M. N. Kobrak and S. A. Rice (unpublished).
- [29] M. Shapiro, Z. Chen, and P. Brumer, Chem. Phys. **217**, 325 (1997).